Solid State Phenomena
ISSN: 1662-9779, Vol. 390, pp 31-38
doi:10.4028/p-LwDCV7

Submitted: 2025-12-19
Revised: 2026-02-24
Accepted: 2026-02-25
Online: 2026-04-17

Empirical Modelling of the Cold Crystallization of PLA

EL HAJJ SLEIMAN Ghinwa[1,2,a*], LABALEC Ewen[2,b], COLOMINES Gaël[2,c]

[1]Icam School of Engineering, 35 av. Champ de Manœuvres, 44470 Carquefou, France

[2]Nantes Université, UMR CNRS 6144, Laboratoire GEPEA, F-44000 Nantes, France

[a]ghinwa.el-hajj-sleiman@icam.fr, [b]ewen.labalec@gmail.com, [c]gael.colomines@univ-nantes.fr, (*corresponding author)

Keywords: Cold crystallization, PLA, empirical modelling.

Abstract. Polylactic acid (PLA) has emerged as a promising alternative to conventional petroleum – based plastics due to its biodegradability, renewable sourcing, and lower environmental impact. However, PLA exhibits a slow crystallization kinetics compared to other semi-crystalline polymers, such as polyethylene (PE) or polypropylene (PP), resulting in an amorphous structure after processing. This amorphous morphology can adversely influence the mechanical properties and overall performance of PLA components. The present study investigates the cold crystallization behavior of PLA using Differential Scanning Calorimetry (DSC) with the objective of developing an empirical model capable of describing crystallinity as joint function of holding temperature and time. The resulting model is intended to serve as a practical reference for industrial applications, facilitating improved control of PLA's microstructure and mechanical performance.

Introduction

Polylactic Acid (PLA) is a widely used biodegradable polymer derived from renewable resources, making it an attractive alternative to petroleum-based plastics. PLA has garnered significant attention in various applications, such as packaging, biomedical devices, and 3D printing, due to its biocompatibility and eco-friendly nature. However, despite its promising potential, PLA exhibits relatively poor crystallization behavior, which limits its thermal mechanical properties, such as strength, rigidity, and thermal stability. One of the key challenges in optimizing PLA's properties for practical applications lies in understanding and controlling its crystallization behavior.

Cold crystallization is a phenomenon that occurs when an amorphous polymer, like PLA, is heated above its glass transition temperature (Tg) but below its melting temperature (Tm), causing crystallization to take place without prior nucleation. This process is particularly relevant in PLA, as it can significantly enhance its mechanical and thermal properties. The rate and extent of cold crystallization in PLA are influenced by various factors, including molecular weight, cooling rate, processing conditions, and the presence of additives and fillers [1].

Long Yu et al. [2] have studied the cold crystallization and the postmelting crystallization of PLA using a high-pressure differential scanning calorimetry (DSC). They have shown that cold crystallization of PLA happened around 70°C. However, this temperature (Tcc) as well as the size of the cold crystallization exotherms decreased with increasing pressure. Omaima Alhaddad et al. [3] have shown in their study that crystallization behaviors of neat PLA depend on the heating rate. The cold crystallization temperature (Tcc) for all values shifted to higher temperatures as the heating rate increased and the peak height simultaneously increased. Ingrid et al. [4] investigated non-isothermal cold crystallization kinetics of PLA compounds. In their study, they applied Ozawa & Mo model [5] which described successfully the experimental data.

Several studies have reported the used of modified Avrami model [6] to describe the non-isothermal crystallization kinetics of PLA samples [7], [8], [9], [10]. Jeziorny [11] proposed that the k_t parameter in the Avrami model should be corrected to account for the heating rate.

In this study, we examine the cold crystallization behavior of PLA and develop an empirical model to describe its crystallization kinetics, with the objective of enhancing the attainable crystallinity. The model couples a sigmoidal arctangent temperature dependence with a Gaussian time-efficiency

factor. While the formulation is empirical rather than mechanistic, it accurately reproduces measured trends and generates a practical response surface suitable for processing optimization and design.

Materials and Methods

Materials

The PLA used in this study is PLI 005 supplied by NATUREPLAST [12] in the form of granulates. The properties of the PLA are presented in the following Table 1:

Table 1. Properties of PLI 005 (NATUREPLAST)

Density [kg/m3]	1250
MFI [190°C; 2.16 kg]	25-35
Shrinkage during molding [%]	0.3-0.4
Glass transition temperature [°C]	60 ± 1.2
Melting temperature [°C]	170-180
Young's modulus [MPa]	3500
Drying time [h]	3
Drying temperature [°C]	60

Characterization methods

Differential Scanning Calorimetry (DSC) measurements were carried out using a Mettler Toledo instruments DSC1 STARe System under a nitrogen atmosphere (50 mL/min). The PLA samples were equilibrated isothermally at 5°C for 10 minutes to ensure thermal stability, followed by heating to 220°C at a rate of 5°C/min, subsequent cooling at a rate of 10°C/min to 5°C, and a second heating cycle to 220°C at a rate of 5°C/min to evaluate thermal transitions associated with melting and recrystallization.

Empirical modelling of cold crystallization

Initial measurements performed at a range of isothermal holding temperatures were used to determine the onset of cold crystallization and to identify the holding times required to achieve complete crystallinity. Although the expected temperature range for pure PLA is typically 80–85 °C, our results indicate deviations from this behavior.

As shown in Fig. 1, a pronounced increase in crystallinity occurs around a threshold temperature of approximately 75 °C. Above this point, a gradual rise in the crystalline fraction is observed, followed by a plateau beyond 90 °C.

Base on the experimental results presented in Fig. 1, the crystallinity as a function of temperature exhibits behavior which can be described by Eq. 1. In fact, the function arctan(x) naturally generates a smooth S-shaped curve because it is monotonically increasing. As $x \to -\infty$, $\arctan(x) \to -\frac{\pi}{2}$, and as $x \to +\infty$, $\arctan(x) \to \frac{\pi}{2}$, with an inflection point located at x=0. [13]

$$\tau_{t\infty}(T) = \frac{\tau_\infty - \tau_0}{\pi} \arctan\left(k^{-1}(T - T_T)\right) + \frac{\tau_\infty + \tau_0}{2} \quad (1)$$

However, in Eq. 1, the lower/ upper asymptotes, the inflection point as well as the steepness factor are represented below:

$\tau_{t\infty}(T)$: Crystallization rate (%) for a given temperature (°C)

τ_∞: Crystallization rate for an infinite temperature (upper asymptotic value)

τ_0: Crystallization rate for a non-crystallized sample at room temperature, or residual crystallization rate (%) (lower asymptotic value)

T_T: The transition temperature from a quasi-amorphous state to a crystalline state (°C) (inflection point)

k: a parameter that represents the rapidity of a transition from one to another (°C) (controls the steepness of the transition)

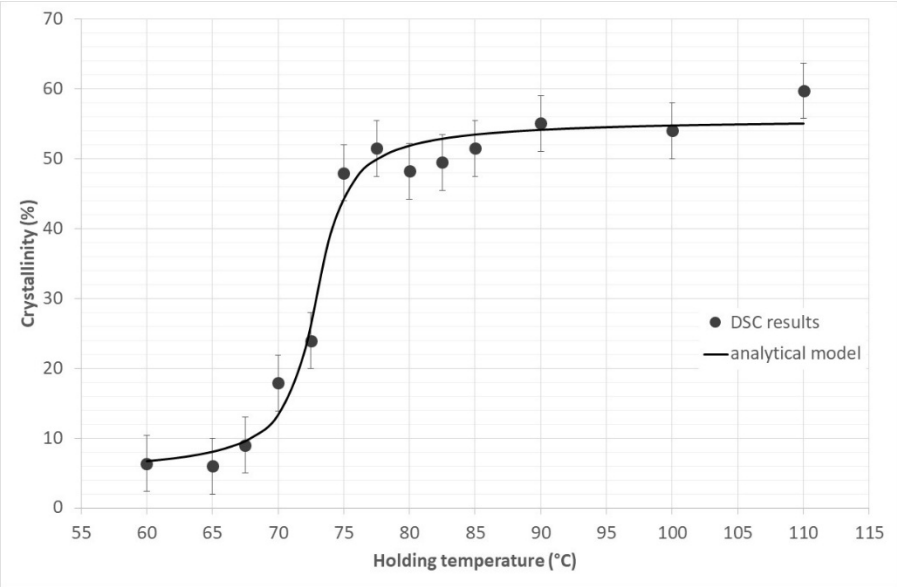

Fig. 1. Measurement of the degree of crystallinity

The model parameters of Eq.1 were estimated using the Solver tool in Microsoft Excel by minimizing the sum of squared residuals. It is important to note that τ_∞ does not account for the melting process occurring around 160–170 °C.

Although this model has no direct physical meaning and serves only as a mathematical description of the phenomenon, the lower and upper plateaus it exhibits are physically consistent. Below the glass transition temperature, the crystallinity remains unchanged because the material is in a glassy state. Likewise, once a certain temperature is exceeded, the crystallinity no longer increases, indicating that the maximum achievable crystalline fraction has been reached. It is also expected that above a specific temperature cold crystallization ceases altogether; however, this threshold could not be identified within the scope of this study due to time limitations.

Within the framework of modeling crystallinity as a function of temperature and time, the minimum holding time required to achieve complete crystallization was determined from DSC data, based on the crystallinity curves obtained at different isothermal temperatures (Fig. 2).

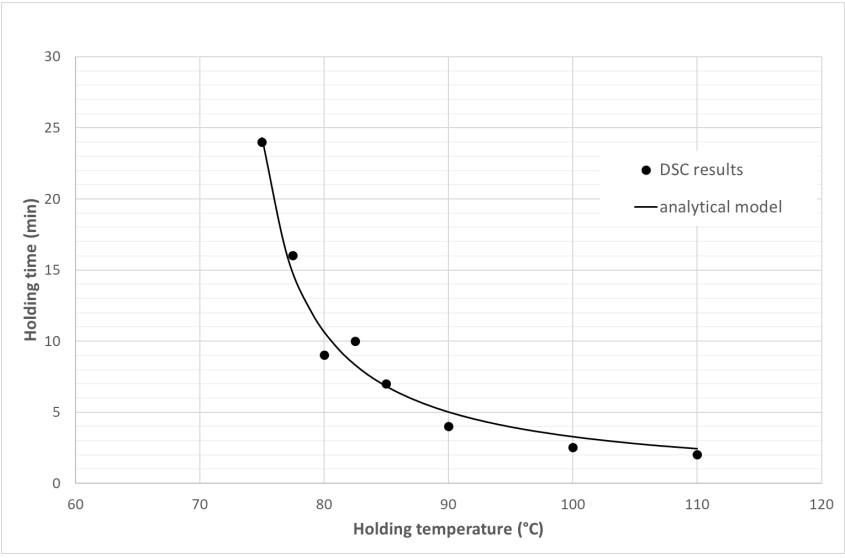

Fig. 1. Holding time required for complete crystallization

It is observed that the holding time required for the transformation to reach a chosen completion level ‘p’ is inversely proportional to the temperature. Eq. 2 describes the temperature dependence of the time required to achieve complete crystallization at a given holding temperature. In the equation, “r” is a kinetic fitting parameter related to the crystallization rate, and “$T_{T,}$” represents a characteristic

temperature associated with the onset of crystallization. The inverse dependence on $(T - T_{T,})$ reflects the strong slowdown of crystallization kinetics as the isothermal temperature approaches $T_{T,}$. The model parameters of Eq. 2 were also estimated using the Solver tool in Microsoft Excel by minimizing the sum of squared residuals.

$$t_{\tau p\%}(T) = \frac{r}{T - T_{T,}} \tag{2}$$

Eq. 1 and Eq. 2, which describe the crystallinity as a function of temperature at infinite time and the minimum holding time required for complete crystallization as a function of holding temperature, respectively, enable the construction of an analytical model describing the degree of crystallization of PLA as a function of both holding temperature and holding time.

The first in constructing the model consists of characterizing the melting transformation, which reflects the crystalline fraction of the material, with crystallinity being quantified through the melting enthalpy. The heat flow associated with melting can be described by a Gaussian function, which reproduces the bell-shaped peak observed in the DSC thermograms (Fig. 3).

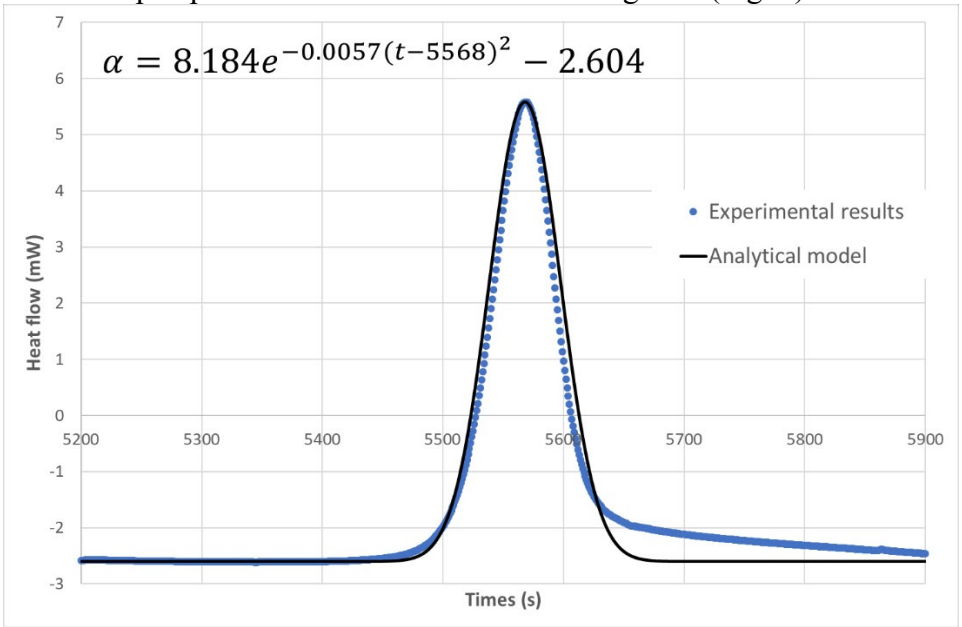

Fig. 2. Modelling of the transformation

This Gaussian function can be represented by a peak of amplitude A, width σ, and position v, as shown in Eq. 3.

$$\alpha(t) = Ae^{-\sigma(t-v)^2} \tag{3}$$

α(t): the heat flow released during the transformation, as a function of time (W)
A: the peak amplitude of the signal (W)
σ: a parameter related to the kinetics of transformation. It controls the width of the distribution (s^{-2})
t: the time elapsed since the start of the transformation (s)
v: the time at which the released power is maximum, in other words the peak position (s)

Due to the properties of Gaussian curves, the released power is positive over an infinite time interval. In reality, however, the transformation occurs over a finite time. To address this, an arbitrary transformation percentage p, 98%, is defined to represent the point at which the transformation is considered complete (Fig. 4).

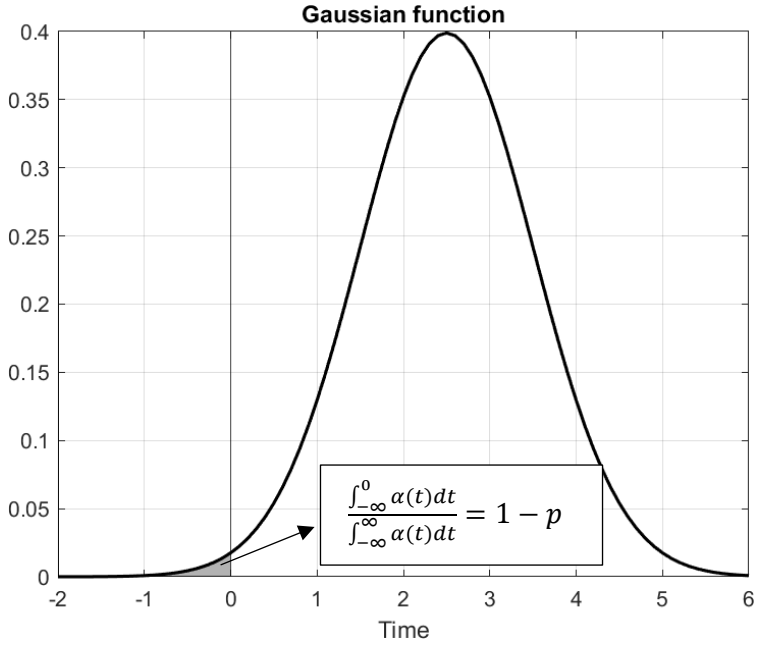

Fig. 3. Arbitrary truncation of the curve representing the transformation

Consequently, at time t=0 s, a very small percentage, 1-p, of the transformation has already occurred. We therefore seek the value of v such that: $\frac{\int_{-\infty}^{0}\alpha(t)dt}{\int_{-\infty}^{\infty}\alpha(t)dt}=1-p$

The integral of a Gaussian over the entire domain is:

$$\int_{-\infty}^{\infty}\alpha(t)dt=\int_{-\infty}^{\infty}Ae^{-\sigma(t-v)^2}dt=A\sqrt{\frac{\pi}{\sigma}}$$

Using the error function, which is a mathematical function that calculated the area under the curve of the Gaussian function from 0 to x, we get:

$$\int_{-\infty}^{0}\alpha(t)dt=\frac{A}{2}\sqrt{\frac{\pi}{\sigma}}\left(1+erf\left(-v\sqrt{\sigma}\right)\right)=\frac{A}{2}\sqrt{\frac{\pi}{\sigma}}\left(1-erf\left(-v\sqrt{\sigma}\right)\right)$$

Thus, the value of v is (Eq. 4):

$$\frac{\int_{-\infty}^{0}\alpha(t)dt}{\int_{-\infty}^{\infty}\alpha(t)dt}=\frac{\frac{A}{2}\sqrt{\frac{\pi}{\sigma}}\left(1-erf\left(-v\sqrt{\sigma}\right)\right)}{\frac{A\sqrt{\pi}}{\sqrt{\sigma}}}=1-p$$

$$\frac{1}{2}\left(erf\left(v\sqrt{\sigma}\right)-1\right)=p-1$$

$$v=\frac{erf^{-1}(2p-1)}{\sqrt{\sigma}} \quad (4)$$

We therefore choose to analyze the transformation over the time interval t∈[0,2v]. Considering that the holding time $t_{(p\%)}$ required to reach a transformation of p% corresponds to this interval, we then obtain the Eq. 5:

$$t_{\tau p\%}=2v=\frac{2\,erf^{-1}(2p-1)}{\sqrt{\sigma}}=\frac{r}{T-T_{T'}} \quad (5)$$

It is therefore possible to express the concentration of the transformation, σ, as a function of temperature T, and we obtain (Eq. 6):

$$\sigma=\left(\frac{2\left(T-T_T'\right)erf^{-1}(2p-1)}{r}\right)^2 \quad (6)$$

Now that the transformation α is properly characterized as a function of temperature and of the running time, we define an efficiency factor η, which represents the normalized cumulative Gaussian starting at t = 0. This factor is defined by Eq. 7:

$$\eta(t) = \frac{\int_0^t \alpha(t)dt}{\int_0^\infty \alpha(t)dt} \tag{7}$$

By integrating $\int_0^t \alpha\,(t)dt$, we get:

$$\int_0^t \alpha\,(t)dt = \frac{A}{2}\sqrt{\frac{\pi}{\sigma}}\left[\mathrm{erf}\left((t-v)\sqrt{\sigma}\right) + \mathrm{erf}\left(v\sqrt{\sigma}\right)\right]$$

Integrating $\int_0^\infty \alpha(t)dt$, we get:

$$\int_0^\infty \alpha(t)dt = \frac{A}{2}\sqrt{\frac{\pi}{\sigma}}\left[\mathrm{erf}\left(v\sqrt{\sigma}\right) + 1\right]$$

Hence, the efficiency factor becomes (Eq. 8):

$$\eta(t) = \frac{\mathrm{erf}\left((t-v)\sqrt{\sigma}\right)+\mathrm{erf}\,(v\sqrt{\sigma})}{\mathrm{erf}\left(v\sqrt{\sigma}\right)+1} \tag{8}$$

To simplify the calculation, erf(x) is approximated by tanh(x/a), with $a = \frac{\sqrt{\pi}}{2}$. However, tanh(x) can be converted to an exponential form, $\tanh(x) = \frac{e^{2x}-1}{e^{2x}+1}$. The factor, η, becomes (Eq. 9):

$$\eta(t) = \frac{\exp\left(2(t-v)a^{-1}\sqrt{\sigma}\right)-\exp\left(-2va^{-1}\sqrt{\sigma}\right)}{\exp\left(2(t-v)a^{-1}\sqrt{\sigma}\right)+1} \tag{9}$$

Now, to express the crystallinity in relative terms, Eq. 1 was normalized between its two asymptotic limits τ_0 and τ_∞. The relative crystallinity rate was defined as in Eq. 10:

$$\tau_r(T) = \frac{\tau_{t\infty}(T)-\tau_0}{\tau_\infty-\tau_0} \tag{10}$$

Which ensures that $\tau_r = 0$ when $\tau_{t\infty} = \tau_0$ and $\tau_r = 1$ when $\tau_{t\infty} = \tau_\infty$. By substituting Eq. 1 in Eq. 10, the relative crystallinity rate equation becomes (Eq. 11):

$$\tau_r(T) = \frac{1}{\pi}\arctan\left(k^{-1}(T - T_T)\right) + \frac{1}{2} \tag{11}$$

By multiplying the relative crystallinity rate (Eq. 11) by the efficiency factor (Eq. 9), we therefore obtain a measurement between 0 and 1 of the crystallinity rates of PLA as a function of the heating temperature and the holding time at this heating temperature. To transform the scale from 0 to 1 on the interval [0; ∞], we multiply by $\tau_\infty - \tau_0$ and we add τ_0. We find (Eq. 12):

$$\tau(T,t) = \Delta\tau.\,\eta\tau_r + \tau_0 \tag{12}$$

In order to model a complete crystallization, we consider p=98%, then we substitute v and σ with their corresponding equations. Thus Eq. 12 becomes (Eq. 13):

$$\tau(T,t) = \Delta\tau\frac{2\arctan\left(k^{-1}(T - T_T)\right) + \pi}{2\pi}\frac{\exp(\gamma c_1) - 1}{\exp(\gamma c_1) + c_2} + \tau_0 \tag{13}$$

Where: $\gamma = (T - T_{T'})t$, while c1 and c2 includes all the constants present in the previous equations. The parameters listed below were determined using Microsoft Excel Solver by minimizing the sum of squared residuals.

$\Delta\tau$ = 48.88% k = 0.9477 (°C) T_T = 72.89 (°C) $T_{T'}$ = 70.88 (°C)

c_1 = 0.07093 ($°C^{-1}.min^{-1}$) c_2 = 33.1890 (unitless) τ_0 = 5.67 (%)

Based on this model, we obtain iso-holding time lines and iso-crystallinity lines in function of temperature and holding time.

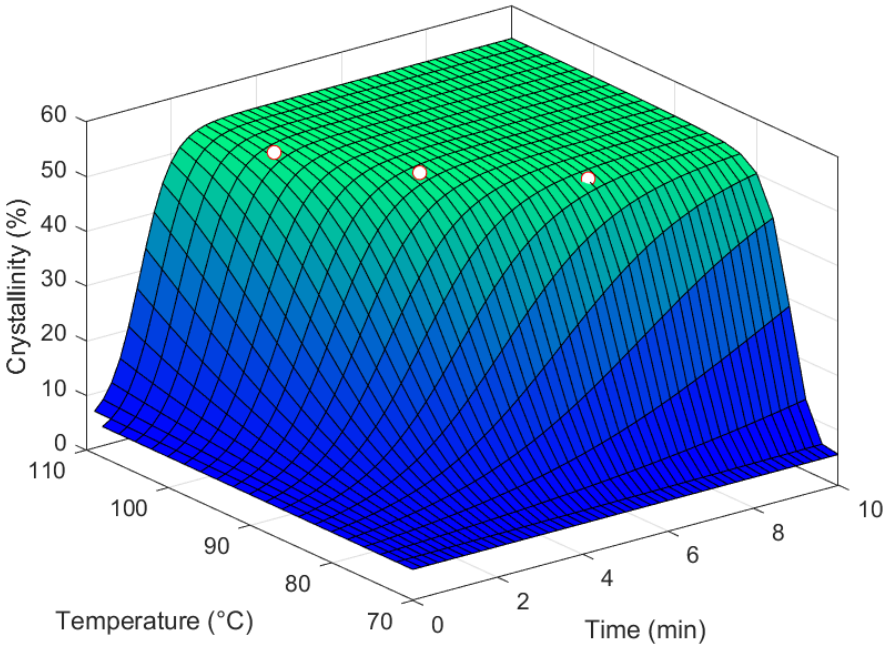

Fig. 4. Representative surface of the crystallinity model

In Fig. 5, three experimental data points (shown in white) were added to assess the validity of the developed analytical model in describing the crystallization behavior. The comparison indicates good agreement, suggesting that the model provides a reliable prediction of the crystallization process.

Conclusion

Differential Scanning Calorimetry (DSC) measurements were performed to characterize cold crystallization behavior of PLA under different heating temperatures. Based on the DSC results, an empirical model was developed to describe the evolution of cold crystallinity of PLA as a function of both the heating temperature and the isothermal holding time. From this model, a representative crystallinity response surface was established, enabling the prediction of the crystallization behavior over a range of processing conditions.

References

[1] E. Tarani et al., “Cold crystallization kinetics and thermal degradation of pla composites with metal oxide nanofillers,” Applied Sciences (Switzerland), vol. 11, no. 7, p. 3004, Apr. 2021.

[2] L. Yu, H. Liu, K. Dean, and L. Chen, “Cold crystallization and postmelting crystallization of PLA plasticized by compressed carbon dioxide,” J. Polym. Sci. B Polym. Phys., vol. 46, no. 23, pp. 2630–2636, Dec. 2008.

[3] O. Alhaddad, S. H. El-Taweel, and Y. Elbahloul, “Nonisothermal cold crystallization kinetics of poly(lactic acid)/bacterial poly(hydroxyoctanoate) (PHO)/talc,” Open Chem., vol. 17, no. 1, pp. 1266–1278, Jan. 2019.

[4] I. D. dos Santos Silva et al., “An investigation of PLA/Babassu cold crystallization kinetics,” J. Therm. Anal. Calorim., vol. 141, no. 4, pp. 1389–1397, Aug. 2020.

[5] R. M. R. Wellen and E. L. Canedo, “Nonisothermal melt and cold crystallization kinetics of poly(3-hydroxybutyrate) and poly(3-hydroxybutyrate)/carbon black compounds. Evaluation of Pseudo-Avrami, Ozawa, and Mo models,” J. Mater. Res., vol. 31, no. 6, pp. 729–739, Mar. 2016.

[6] M. Avrami, “Kinetics of Phase Change. II Transformation-Time Relations for Random Distribution of Nuclei,” J. Chem. Phys., vol. 8, no. 2, pp. 212–224, Feb. 1940.

[7] Z. Su, W. Guo, Y. Liu, Q. Li, and C. Wu, “Non-isothermal crystallization kinetics of poly (lactic acid)/modified carbon black composite,” Polymer Bulletin, vol. 62, no. 5, pp. 629–642, May 2009.

[8] P. N. Tri, S. Domenek, A. Guinault, and C. Sollogoub, “Crystallization behavior of poly(lactide)/poly(β-hydroxybutyrate)/talc composites,” J. Appl. Polym. Sci., vol. 129, no. 6, pp. 3355–3365, Sep. 2013.

[9] M. Li, D. Hu, Y. Wang, and C. Shen, “Nonisothermal crystallization kinetics of poly(lactic acid) formulations comprising talc with poly(ethylene glycol),” Polym. Eng. Sci., vol. 50, no. 12, pp. 2298–2305, Dec. 2010.

[10] V. H. Sangeetha, R. B. Valapa, S. K. Nayak, and T. O. Varghese, “Investigation on the Influence of EVA Content on the Mechanical and Thermal Characteristics of Poly(lactic acid) Blends,” J. Polym. Environ., vol. 26, no. 1, pp. 1–14, Jan. 2018.

[11] A. Jeziorny, “Parameters characterizing the kinetics of the non-isothermal crystallization of poly(ethylene terephthalate) determined by d.s.c.,” Polymer (Guildf)., vol. 19, no. 10, pp. 1142–1144, Oct. 1978.

[12] “Natureplast PLI 005 | Agrobiobase, la vitrine des produits biosourcés.” https://www.agrobiobase.com/fr/annuaire/bioproduits/plastiques-composites-caoutchouc/natureplast-pli-005

[13] “Fonction Arctangente [Fonctions usuelles et leurs réciproques].” https://uel.unisciel.fr/mathematiques/analyse3/analyse3_ch02/co/apprendre_ch02_23.html